RAPID COMMUNICATION

Nano-structured non-platinum catalysts for automotive fuel cell application

Alexey Serov[a], Kateryna Artyushkova[a], Ellazar Niangar[b], Chunmei Wang[b], Nilesh Dale[b], Frederic Jaouen[c], Moulay-Tahar Sougrati[c], Qingying Jia[d], Sanjeev Mukerjee[d], Plamen Atanassov[a,*]

[a]Chemical & Biological Engineering Department, Center for Micro-Engineered Materials, University of New Mexico, Albuquerque, NM 87131, United States
[b]Zero Emission Research, Fuel cell and Battery Laboratory, Nissan Technical Center North America, Farmington Hills, MI 48331, United States
[c]Institut Charles Gerhardt de Montpellier, UMR 5253 CNRS - Université de Montpellier, Agrégats, Interfaces et Matériaux pour l'Energie, 2 Place Eugène Bataillon, 34095 Montpellier cedex 5, France
[d]Department of Chemistry and Chemical Biology, Northeastern University, 364 Egan Research Center, 360 Huntington Avenue, Boston, MA 02115, USA

Abstract
A highly active and durable non-platinum group metal (non-PGM) electrocatalyst was synthesized at high temperature from a catalyst precursor involving a ferrous iron salt and a nitrogen-containing charge-transfer salt as a precursor to form a nano-structured catalyst with performance level that makes it suitable for automotive applications. Such precursors have not been previously investigated for non-PGM catalysts. The synthesized material belongs to the class of metal-nitrogen-carbon catalysts and possesses an open-frame structure controlled by the silica-templating synthesis method. Thorough characterization using X-ray photoelectron, Mössbauer and in situ X-ray absorption spectroscopies demonstrates the successful formation of FeN_xC_y moieties that are active towards the oxygen reduction reaction. We report high kinetic current densities and high power performance in both rotating disk electrode and membrane

*Corresponding author.
  E-mail address: plamen@unm.edu (P. Atanassov).

electrode assembly studies. This Fe-N-C catalyst, jointly investigated by academic and industry partners, has shown high durability under different protocols, including that defined by the US Department of Energy Durability Working Group and Nissan's load cycling protocol. In summary, the present Fe-N-C catalyst is highly active and durable, making it a viable alternative to Pt-based electrocatalysts for automobile fuel cell applications.

Introduction

Leading automobile manufacturers just launched the commercialization of zero-emission fuel cell electric vehicles (FCEVs) [1-3]. At the moment, all state-of-the art vehicle stacks use platinum-based electrocatalysts on both sides of the membrane electrode assembly (MEA). The MEA and Pt electrocatalyst contribute 40-50% of the total stack price [4], resulting in high FCEV costs and affecting its market introduction. For successful commercialization of FCEVs, the amount of platinum in the stack should be substantially reduced, ideally down to zero with non-platinum group metal (non-PGM) catalysts.

Recently, several research groups have reported significant progress in the synthesis of highly active and durable non-PGM cathode catalysts [5-9]. These catalysts contain transition metals (M) coordinated by nitrogen (N) inside a carbon matrix (C) and are symbolized as M-N-C catalysts. Non-templated synthetic approaches involve either (i) the dispersion of M and N precursors on pre-existing carbon supports, or (ii) one-pot synthesis approach with M, N and organic or metal–organic precursors [5]. Complementary to these synthesis approaches, a templated synthesis approach allows for the design of hierarchically-structured materials resulting in catalysts with an *open-frame morphology*. The group at University of New Mexico (UNM) introduced the sacrificial support method (SSM) and applied it to the templated syntheses of both PGM [10] and non-PGM catalysts [11-19].

The SSM was successfully used for the preparation of several classes of M-N-C catalysts for oxygen reduction based on macrocycles [12], low molecular weight [11,13-15,18] and polymeric [17] precursors. This method allows a high level of control on the catalysts surface area and its pore size distribution trough the fidelity of the template. These parameters affect water management and reactant gas transport within the catalyst layer of fuel cell MEAs and are therefore crucial for obtaining superior MEA performance and durability. The nitrogen-carbon precursors of choice at UNM contain hetero-atomic nitrogen and amino groups [5-9,13,15,18]. We describe here the properties and structure of a Fe-N-C catalyst synthesized from nicarbazin (NCB), a charge-transfer organic salt. To the best of our knowledge, charge transfer salts have not been previously used in the synthesis of M-N-C catalysts. This catalyst shows high activity and durability and is therefore a promising candidate for future polymer electrolyte membrane fuel cell stacks.

Vehicle stack operation conditions (humidity, back pressure, etc.) put specific requirements on the design of cathode materials. Our recent generation of catalysts was mainly developed for passive (air-breathing) cathodes for portable fuel cell applications [11-13,15,18]. In order to meet automobile specifications, we have optimized the SSM to (i) increase the number of defects and, therefore, the dispersion of active sites in the graphene nano-sheets, (ii) ensure integration of Nafion® with the Fe-containing, nicarbazin-derived (Fe-NCB) catalysts, (iii) and improve the water management by providing a material with appropriate physico-chemical properties suitable for integration in membrane electrode assembly (MEA).

A modified sacrificial support method (SSM) was used to synthesize this novel catalyst from iron and charge-transfer salt (nicarbazin) precursors (Figure 1). As a sacrificial support, we have selected medium-surface area Cab-O-Sil®
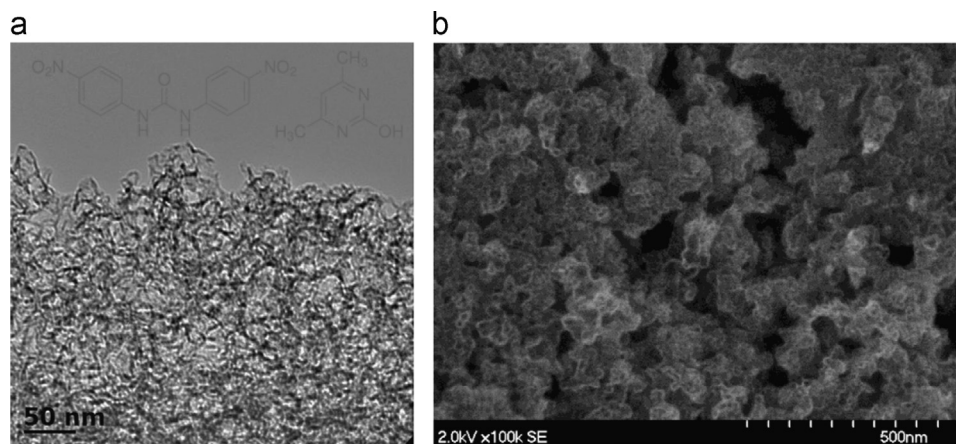

Figure 1 TEM (a) and SEM (b) images for the Fe-NCB catalyst synthesized at $T=900$ °C in N_2 for X minutes with Fe:NCB ratio 1:8, second heat treatment at $T=950$ °C for 30 min in NH_3. Inset in (a) the chemical formula of the charge-transfer salt, nicarbazin.

fumed silica. Iron and nicarbazin precursors were intimately mixed with the fumed SiO_2 particles followed by high temperature heat treatment in a nitrogen atmosphere. After the pyrolysis step, HF leaching was used to remove the sacrificial support (silica) and unreacted iron species (metal iron particles and/or iron oxides). A second pyrolysis in a reactive atmosphere (NH_3) was then performed to remove volatile HF-derived species, to introduce additional surface defects, and to extend the open-pore structure created by the removal of the sacrificial support. SEM images in Figure 1 show that the Fe-NCB catalyst has several levels of porosity originating from the removal of SiO_2 nanoparticles and from morphological defects formed during the decomposition of nicarbazin at high-temperature. TEM imaging (Figure 1) shows an open structure with uniform morphological units. High resolution TEM (Figure 1, inset) shows graphitic planes along with an amorphous carbon phase. While EDS analysis confirmed the presence of Fe, Fe-based particles could not be observed in the TEM images, suggesting that iron particles are absent or that they are extremely small and homogeneously throughout the nitrogen-enriched carbon network.

X-ray photoelectron spectroscopy (XPS) detected 4.7 at% of nitrogen and approximately 0.4 at% of iron, values typically observed for M-N-C electrocatalysts synthesized in our group (Figure S1, Supporting information) [18]. The presence of a significant amount of pyridinic nitrogen (established from the XPS binding energy at 398.8 eV) as well as substantial amount of nitrogen associated with Fe (interpreted as Fe-N_x centers and observed at a binding energy of 399.6 eV) is important, as these chemical moieties were previously linked to high activity of M-N-C electrocatalysts [14,20-23]. High resolution Fe 3d spectra confirmed the presence of various types of oxides, small amount of Fe–Fe or Fe–C moieties and, more importantly, the substantial presence of Fe coordinated to N.

Iron speciation in the Fe-NCB catalyst was further characterized with ^{57}Fe Mössbauer spectroscopy (Figure 2). This technique is well suited for the investigation of even minuscule modifications in the energy levels of iron nuclei resulting from interactions with the electronic orbitals, down to 1 part to 10^{10}. Three types of nuclear-electronic interactions exist, i.e. electric monopole, electric quadrupole and magnetic dipole interactions, leading to a singlet, doublet, and sextet in the absorption spectrum, respectively. As was
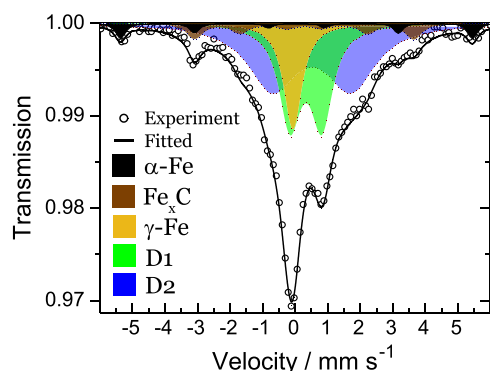
Figure 2 Mössbauer absorption spectrum and its deconvolution for the Fe-NCB catalyst synthesized at 900 °C and second heat treatment in NH_3 at 950 °C. The measurement was performed at room temperature and calibrated vs. α-Fe foil.

reported before and as confirmed by XPS in this study, iron-based catalysts synthesized at high temperatures comprise a plurality of iron species that have been detected either by Mössbauer, XPS or X-ray absorption spectroscopy [23-26]. Five Fe species are clearly identified in the Fe-NCB catalyst resulting in a singlet, two doublets (D1 and D2) and two sextets (Figure 2). The Mössbauer parameters of each component are shown in Table 1. The singlet is assigned to either γ-Fe or super-paramagnetic Fe nanoparticles [23], D1 and D2 are assigned to a four-fold nitrogen or nitrogen-carbon coordination of Fe^{II} in low-spin (LS) and medium-spin state (MS), respectively [23,25,26], while the sextet's parameters match those of α-Fe and iron carbide. The assignments of D1 and D2 are subject of ongoing research related to the exact site structure and to the integration of FeN_4 or FeN_2C_2 moieties, which can be viewed either at defect sites within a graphene layer (edge defects), or as a structure bridging two graphene zigzag- or armchair-edges. The metallic iron and iron carbide species observed in Fe-NCB must be wrapped in a graphitic layer, otherwise they would have been dissolved during the template etching step in which HF was used. The observed ORR activity is most likely linked to the FeN_x moieties related to the D1 and/or D2 spectroscopic signatures [23,25,26].

The relative content of D1 or D2 is high (Table 1), demonstrating the successful integration of the majority of the iron in FeN_xC_y molecular sites during pyrolysis. The existence of Fe-N coordination revealed by Mössbauer spectra, (doublets) is also supported by the Fe-N binding energy in XPS at 399.6 eV [22]. From several Mössbauer studies on Fe-N-C-catalysts synthesized through various approaches, a positive correlation between the ORR activity and the absolute content of the D1 species has emerged [22,24,26]. In fact, the Mössbauer parameters of D1 are similar to those of Fe^{II}-phthalocyanine (Fe^{II}Pc) adsorbed on carbon supports, in which the initially planar FeN_4 coordination of Fe^{II}Pc interacted with the electronic support [27]. In addition, the smaller width of the Lorentzian line used for D1 than for D2 (0.8 and 1.83 mm s^{-1}, respectively; see Table 1) suggests a better definition of the site structure for D1 and a plurality of structures for D2 [25]. Knowing the Fe-content of the catalyst (1-2 wt%), quantification of all Fe-species is possible from their relative Mössbauer absorption area. The combined 26% relative area of α-Fe, Fe_xC and γ-Fe (Table 1) expectedly accounts for approximately 10% of the relative Fe content of the catalyst due to larger Lamb Mössbauer factors for crystalline iron species than for molecular iron species.

The local atomic structure of the Fe species in the Fe-NCB catalyst under operating conditions was further probed using in situ X-ray absorption spectroscopy (XAS). Traditional Fourier Transform (FT) EXAFS analysis up to the second shell is applied at the Fe K edge for representative data collected at 0.3 and 0.9 V vs. RHE (Figure 3). As per norms typically associated with EXAFS analysis, statistically unique solutions were obtained for EXAFS parameters (Table 2). These are exemplified by excellent fits obtained for the phase and amplitude parameters using in situ experimental data and model parameters.

The two FT peaks displayed in the left of Figure 3 clearly confirm the plurality of coordination chemistries in the Fe-NCB catalyst. The second FT peak at ~2.1 Å (all the radial distances given in this work are without phase correction) can be well

Table 1   Mössbauer fitted parameters for the Fe-NCB catalyst.

Component (assignment)	IS (mm s^{-1})	QS (mm s^{-1})	H Tesla	LW (mm s^{-1})	Relative absorption area (%)
α-Fe	0.04	-	33.5	0.37	4
Fe$_x$C	0.29	-	20.2	0.62	8
Param. or γ-Fe	-0.07	-	-	0.67	14
D1 (Fe^{II}N$_4$ LS)	0.33	0.98	-	0.80	30
D2 (Fe^{II}N$_4$ MS)	0.51	2.34	-	1.83	44
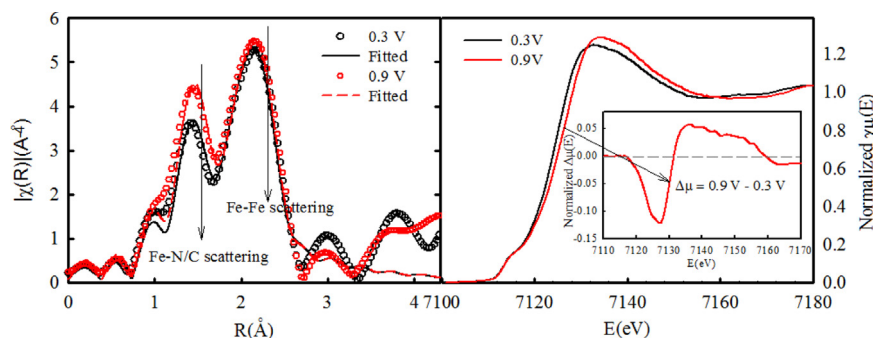
Figure 3   Fourier Transforms of the Fe K edge XAS data and the corresponding EXAFS fit (left), and the XANES spectra (right) together with the $\Delta\mu = \mu(0.90\,\text{V}) - \mu(0.30\,\text{V})$ (inset) of the Fe-NCB catalyst. The measurements were performed at 0.3 and 0.9 V vs. RHE in the N$_2$-saturated 0.1 M HClO$_4$ electrolyte at room temperature.

Table 2   Results of fitting EXAFS data obtained under in situ electrochemical operating conditions for the Fe-NCB catalyst synthesized at 900 °C and second heat treatment in NH$_3$ at 950 °C. The measurements were performed at 0.3 and 0.9 V vs. RHE in the N$_2$-saturated 0.1 M HClO$_4$ electrolyte at room temperature. Coordination number (N), phase-corrected bond length (R), Debye–Waller factor (σ^2), and edge shifts (E_0) are shown for each interaction.

Potential	Fe-C/N/O path				Fe-Fe path			
	CN	R (Å)	σ^2 (Å^2) × 10^{-3}	E_0 (eV)	CN	R (Å)	σ^2 (Å^2) × 10^{-3}	E_0 (eV)
0.3 V	3.6 (7)	2.02 (2)	9 (3)	-5 (1)	1.2 (3)	2.51 (1)	9 (3)	-5 (1)
0.9 V	4.0 (8)	2.01 (2)	4 (2)	-6 (2)	1.3 (3)	2.52 (1)	4 (2)	-6 (2)

fixed at 0.88 as obtained by fitting the iron reference foil. The Fourier-transformed (FT) EXAFS data were fitted under simultaneous $k^{1,2,3}$ weighting, R range 1.0-3.0 Å, k range 1.95-10.96 Å^{-1}. The statistical errors of the least-squares fits were determined by ARTEMIS.

fitted as a Fe-Fe shell with a bond length of ∼2.51 Å. This bond length is close to the Fe-Fe bond length in iron carbide (2.48 Å), confirming that the Fe-NCB catalyst contains some iron carbides that are stable under the acidic and oxidizing environment. The small coordination number for Fe-Fe (CN$_{\text{Fe-Fe}}$ ∼1.2) suggests either that the content of metallic iron particles is small compared to the content of the Fe-N$_x$ species, and/or the size of metallic particles is sufficiently small to result in significant fraction of surface Fe with lower CN. The former hypothesis is confirmed by the small amounts of γ-Fe, α-Fe and Fe$_x$C obtained by Mossbauer and the absence of visible particles in high resolution TEM. The constant peak intensity with the electrochemical potential indicates that the iron carbide is not directly involved in the reaction.
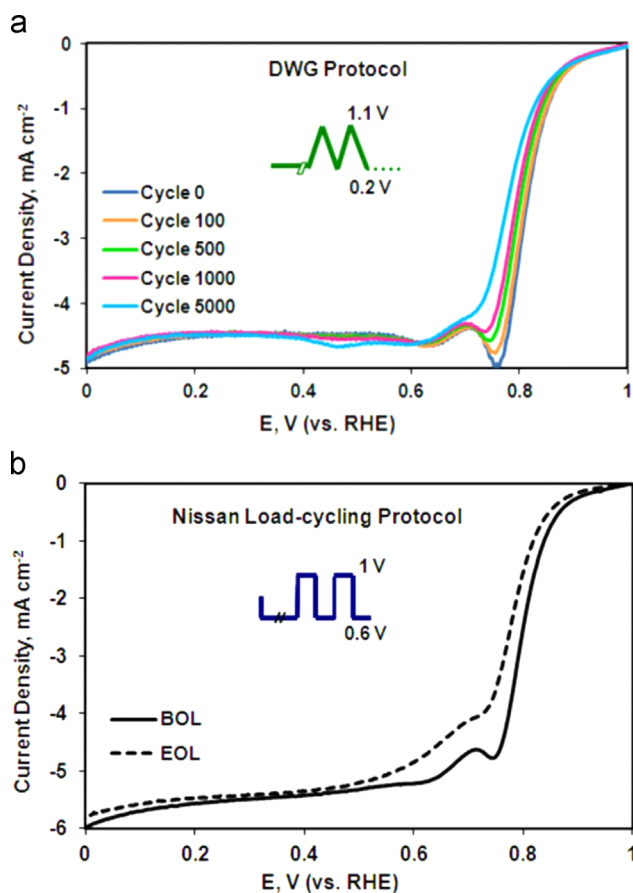
The first FT peak at ∼1.6 Å arises from the Fe-N/Fe-C/Fe-O scattering. Nitrogen, carbon and oxygen atoms cannot be distinguished by XAS due to similar atomic weight. Owing to the bulk averaging nature of the EXAFS technique, the corresponding coordination number at 0.3 V (3.6) is a weighted

average of the coordination number of the Fe-N bonds in the Fe-N$_x$ species and the Fe-C bonds in the iron carbide. As the iron carbide content is relatively low, and the first shell Fe-C coordination number is small (≤ 3), it is reasonable to deduce that the Fe-N coordination number in the Fe-N$_x$ species is 4. The increase in the coordination number as the potential is increased to 0.9 V suggests the adsorption of oxygenated species onto the Fe-N$_4$ sites. These hypotheses are further supported by the $\Delta\mu$ analysis discussed below.

The XANES of the Fe-NCB catalyst at 0.3 and 0.9 V vs. RHE are displayed in Figure 3 (right). For un-pyrolyzed Fe-based macrocycles, the presence of a pre-edge peak at ∼7117 eV is the fingerprint for a FeN$_4$ square-planar coordination [28-30]. Here, the absence of this pre-edge peak in the XANES of Fe-NCB is indicative of the lack of the intact planar Fe-N$_4$ moiety in this catalyst. The XANES edge shifts to higher energy as the potential is increased from 0.3 to 0.9 V, indicating the increase of the Fe oxidation state. The corresponding $\Delta\mu$ signal (inset of Figure 3) is essentially

identical to that obtained on FeTPP/BP pyrolyzed at 800 °C, [30] and can be nicely mimicked by the theoretical $\Delta\mu$ spectrum obtained using the FeN$_4$C$_y$ cluster models with either a partial ($y=10$) or complete destruction ($y=8$) of the carbon methane bridges. In summary, the combination of the EXAFS, XANES, and $\Delta\mu$ analysis suggest that (1) the active sites in this catalyst are formed via the covalent incorporation of Fe-N$_4$ moieties in the di-vacant defective centers on the carbon basal plane ($y=10$) or in armchair edges of two adjacent graphene layers ($y=8$), which have been widely proposed as the active sites in pyrolyzed Fe-based catalysts; [6,30,31]. The Fe^{2+}-N$_4$ active site coordination at 0.3 V undergoes a redox transition to a penta-coordinate $(H)O-Fe^{3+}-N_4$ at 0.90 V, and the adsorption of the (H)O species triggered by the Fe^{2+}/Fe^{3+} redox transition poisons the active sites.

We optimized the pyrolysis process and established that Fe-NCB heat treated at $T=900$ °C for 1 h has the highest activity (Figure S2) with a value of $E_{1/2}=0.8$ V vs. RHE. The number of electrons participating in ORR was calculated using Eq. S1 and was found to be 3.8e$^-$. After optimization, we then synthesized several large batches ($\sim$5 g each) of the Fe-NCB catalyst, which were then tested at Nissan Technical Center North America in order to measure the performance and durability of this catalyst under automotive and durability test conditions that simulate actual stack conditions.

Rotating disk electrode (RDE) measurements at Nissan of a large laboratory batch of the catalyst revealed a high kinetic current density at 0.8 V of $i_k=4.6$ mA cm^{-2} with a Tafel slope of 52 mV/decade (Figure S3). The durability of the catalyst was evaluated using the DOE Durability Working Group (DWG) proposed protocol and Nissan load-cycling protocol (see Figure 4) [32,33]. Under both durability tests, the catalyst presented a drop of the half-wave potential of
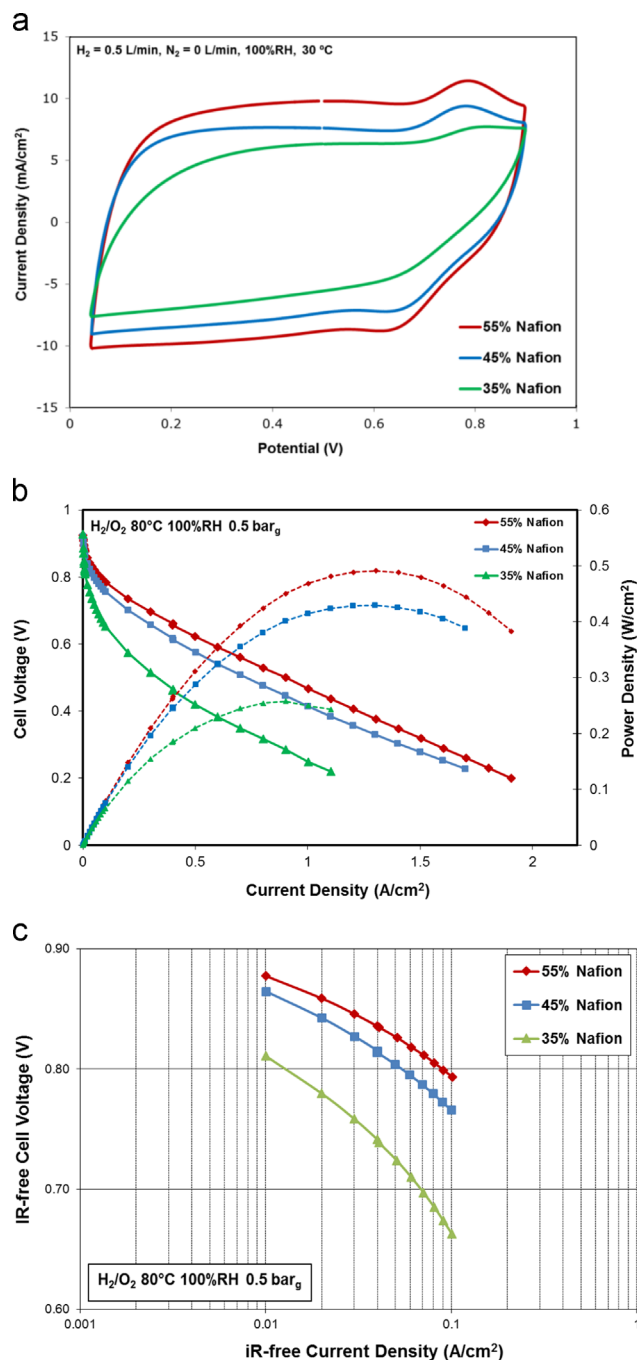
Figure 5 CV (a), MEA performance (b) and kinetic current density (c) of the Fe-NCB catalyst with varying Nafion content. Conditions: $T_{cell}=80$ °C, 100% RH, 0.5 bar back pressure; anode catalyst: Johnson Matthey Fuel Cell (JMFC) 0.4 mg$_{Pt}$/cm^2, an NRE 211 membrane, and cathode Fe-NCB-based catlysts loading of 4 mg$_{catalyst}$/cm^2.

Figure 4 Durability in RDE tests under (A) DWG: 900 RPM and (B) Nissan load-cycling protocols: 1600 RPM. Both in 0.5 M H$_2$SO$_4$ saturated with (A) O$_2$ and (B) N$_2$.

only 3–4% relative to the initial value, which prompted us to further evaluate it in an automotive-type MEA.

MEAs were fabricated and evaluated at Nissan Technical Center North America. Figure 5 shows the CV and MEA performance of the Fe-NCB catalyst under the recommended DOE conditions of H_2/O_2 operation, 100% RH, and 1 bar O_2 partial pressure. Three MEAs with the same catalyst loading of 4 mg/cm^2, but different Nafion® content, were investigated. CV curves of all three MEAs are shown in Figure 5(a) and indicate high capacitance of catalyst due to high surface area. The open circuit voltage (OCV) was 0.92 V and did not change with increasing Nafion® content. Figure 5(b) shows that increasing the ionomer content from 35% to 55% significantly changes the polarization performance. The poor polarization of the 35 wt% Nafion® MEA may be attributed to incomplete Nafion® coverage of the non-PGM active sites. Better ionomer coverage was achieved upon increasing the Nafion® content to 45% and 55% as supported by the significant improvement in the polarization performance. Increasing the ionomer content from 45% to 55% resulted in further increased kinetic currents. As shown in Figure 5(c), the MEA containing the Fe-NCB catalyst with 55% Nafion® gave a kinetic current close to 100 mA cm^{-2} at 0.8 V$_{iR\text{-free}}$ for the catalysts loading of 4 mg/cm^2. This result was reproduced using three MEAs from three different catalyst batches, synthesized at UNM, as shown in Figure S4. The reproducibility of the high current densities obtained with this catalyst is confirmed by the practically overlapping Tafel plots. The use of Nafion® NRE 211 results in substantial reduction of resistive losses and better water management, particularly at low cell voltage and high current density [5].

In summary, this work is the first report of an M–N–C catalyst derived from the pyrolysis of nitrogen containing charge-transfer salt precursors and using the sacrificial support method to obtain a catalyst with an open frame structure. High kinetic current densities and power performance were observed in both RDE and MEA tests. The Fe-NCB catalyst was found to be durable under different test protocols: including that recommended by the US Department of Energy Durability Working Group and Nissan/FCCJ's load cycling protocol. The high performance and excellent durability was independently validated at Nissan North America's Fuel Cell and Battery Laboratory.

The high performance and durability of the catalyst may be related to the successful formation of large amounts of FeN$_x$C$_y$ sites which are active towards oxygen reduction, and the uniform open area morphology with a hierarchy of pores in which these active centers are homogeneously distributed and easily accessible to reactants.

Acknowledgments

Appendix A.   Supporting information

Supplementary data associated with this article can be found in the online version at http://dx.doi.org/10.1016/j.nanoen.2015.07.002.

References

[1] Nissan Press Release ⟨http://www.nissan-global.com/EN/NEWS/2013/_STORY/130128-02-e.html⟩, (January 28, 2013).

[2] Hyundai Press Office ⟨http://www.hyundaipressoffice.co.uk/release/379/⟩.

[3] Toyota Press Office ⟨http://www2.toyota.co.jp/en/news/13/01/0124.html⟩.

[4] ⟨http://hydrogendoedev.nrel.gov/pdfs/progress10/v_a_3_sinha.pdf⟩.

[5] F. Jaouen, E. Proietti, M. Lefevre, R. Chenitz, J.P. Dodelet, G. Wu, H.T. Chung, C.M. Johnston, P. Zelenay, Energy Environ. Sci. 4 (2011) 114-130.

[6] M. Lefevre, E. Proietti, F. Jaouen, J.P. Dodelet, Science 324 (2009) 71-74.

[7] E. Proietti, F. Jaouen, M. Lefevre, N. Larouche, J. Tian, J. Herranz, J.P. Dodelet, Nat. Commun. (2011). http://dx.doi.org/10.1038/Ncomms1427.

[8] G. Wu, K.L. More, C.M. Johnston, P. Zelenay, Science 332 (2011) 443-447.

[9] G. Wu, K.L. More, P. Xu, H.L. Wang, M. Ferrandon, A.J. Kropf, D.J. Myers, S.G. Ma, C.M. Johnston, P. Zelenay, Chem. Commun. 49 (2013) 3291-3293.

[10] A. Falase, M. Main, K. Garcia, A. Serov, C. Lau, P. Atanassov, Electrochim. Acta 66 (2012) 295-301.

[11] S. Brocato, A. Serov, P. Atanassov, Electrochim. Acta 87 (2013) 361-365.

[12] S. Pylypenko, S. Mukherjee, T.S. Olson, P. Atanassov, Electrochim. Acta 53 (2008) 7875-7883.

[13] M.H. Robson, A. Serov, K. Artyushkova, P. Atanassov, Electrochim. Acta 90 (2013) 656-665.

[14] A. Serov, K. Artyushkova, P. Atanassov, Adv. Energy Mater. 4 (2014) 1301735. http://dx.doi.org/10.1002/aenm.201301735.

[15] N.I. Andersen, A. Serov, P. Atanassov, Appl. Catal. B: Environ. 163 (2015) 623-627.

[16] A. Serov, N.I. Andersen, A.J. Roy, I. Matanovic, K. Artyushkova, P. Atanassov, J. Electrochem. Soc. 162 (4) (2015) F449-F454.

[17] A. Serov, M.H. Robson, K. Artyushkova, P. Atanassov, Appl. Catal. B: Environ. 127 (2012) 300-306.

[18] A. Serov, M.H. Robson, M. Smolnik, P. Atanassov, Electrochim. Acta 109 (2013) 433-439.

[19] A. Zalineeva, A. Serov, M. Padilla, U. Martinez, K. Artyushkova, S. Baranton, C. Coutanceau, P. Atanassov, J. Am. Chem. Soc. 136 (2014) 3937-3945.

[20] U.I. Kramm, M. Lefevre, N. Larouche, D. Schmeisser, J. P. Dodelet, J. Am. Chem. Soc. 136 (2014) 978-985.

[21] U. Tylus, Q. Jia, K. Strickland, N. Ramaswamy, A. Serov, P. Atanassov, S. Mukerjee, J. Phys. Chem. C 118 (17) (2014) 8999-9008.

[22] U.I. Kramm, I. Abs-Wurmbach, I. Herrmann-Geppert, J. Radnik, S. Fiechter, P. Bogdanoff, J. Electrochem. Soc. 158 (2011) B69-B78.

[23] U.I. Kramm, J. Herranz, N. Larouche, T.M. Arruda, M. Lefèvre, F. Jaouen, P. Bogdanoff, S. Fiechter, I. Abs-Wurmbach, S. Mukerjee, J.P. Dodelet, PCCP 14 (2012) 11673-11688.

[24] M. Ferrandon, J.A. Kropf, D.J. Myers, K. Artyushkova, U. I. Kramm, P. Bogdanoff, G. Wu, C.M. Johnston, P. Zelenay, J. Phys. Chem. C 116 (2012) 16001-16013.

[25] U.I. Kramm, M. Lefèvre, N. Larouche, D. Schmeisser, J. P. Dodelet, J. Am. Chem. Soc. 136 (2013) 978-985.

[26] A. Morozan, M.T. Sougrati, V. Goellner, D. Jones, L. Stievano, F. Jaouen, Electrochim. Acta 119 (2014) 192-205.

[27] D.A. Scherson, S.B. Yao, E.B. Yeager, J. Eldridge, M. E. Kordesch, R.W. Hoffman, J. Phys. Chem. 87 (1983) 932-943.

[28] M.C.M. Alves, J.P. Dodelet, D. Guay, M. Ladouceur, G. Tourillon, J. Phys. Chem. 96 (1992) 10898-10905.

[29] I.T. Bae, D.A. Tryk, D.A. Scherson, J. Phys. Chem. B 102 (1998) 4114-4117.

[30] N. Ramaswamy, U. Tylus, Q. Jia, S. Mukerjee, J. Am. Chem. Soc. 135 (2013) 15443-15449.

[31] D. Singh, J. Tian, K. Mamtani, J. King, J.T. Miller b, U. S. Ozkan, J. Catal. 317 (3) (2014) 0-43.

[32] ⟨http://www1.eere.energy.gov/hydrogenandfuelcells/m/dur ability_group.html⟩.

[33] A. Ohma, K. Shinohara, A. Iiyama, T. Yoshida, A. Daimaru, ECS Trans. 41 (2011) 775-784.

Alexey Serov (M.S. in Inorganic Chemistry from Moscow State University, and Ph.D. in Physical Chemistry from University of Bern) is a Research Assistant Professor of Chemical & Biological Engineering Department at the University of New Mexico. Dr. Serov research focuses on materials design and characterization for energy applications and includes development of electrocatalyst for fuel cells, electrolyzers and lithium-ion batteries. He is the author of more than 40 peer-reviewed articles and more than 30 issued patents.

Dr. Kateryna Artyushkova obtained her Ph.D. at the Chemistry Department, Kent State University, Kent, Ohio, in 2001 under the supervision of professor Julia E. Fulghum. She was post-doctoral scientists at Chemical and Nuclear Engineering Department at University of New Mexico, focusing on multivariate analysis of spectroscopic and imaging data, image fusion and digital image processing. In 2008, Kateryna Artyushkova has been promoted to research Associate Professor at UNM. She has more than 15 years of experience with all aspects of X-ray photoelectron spectroscopy, including instrumentation, experimental design for optimizing time and information content, and data analysis. Her research focuses on developing methodology for accelerating material design through structure-to-property modeling and characterization of functional materials using ex-situ and in-situ spectroscopic and microscopic techniques.

Dr.Ellazar Niangar (Ely) obtained his Ph.D. in Chemistry from Princeton University in 2011 under the guidance of Prof. Andrew Bocarsly. He then joined Nissan Technical Center North America (NTCNA) as a research associate for fuel cell research. He is currently the technical leader for PEM fuel cell catalyst and catalyst layer development at NTCNA. His research experience includes the synthesis of fuel cell catalysts and catalyst supports, RDE testing, catalyst ink formulation, catalyst layer design and optimization, and thorough MEA performance and durability testing. Ely enjoys working in collaborative projects, and he has contributed to the development of non-carbon supports, non-PGM cathodes, and electrospun nanofiber electrodes while working with Nissan's research partners. In 2015, Ely joined GM's fuel cell research team to work on the development of gas diffusion electrodes.
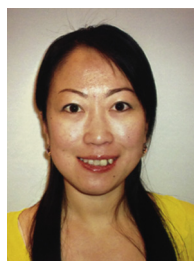
Dr.Chunmei Wang obtained her Ph.D. at the Pennsylvania State University in Energy and Environmental Engineering in 2010. She joined in Nissan Technical Center North America as a research associate in fuel cell research after her graduation. Since 2014, she is working at Ford Motor Company as a Fuel Cell Research Engineer. Currently, Chunmei is leading the efforts on the fuel cell stack development and system investigation. She has more than twenty publications in International Scientific Journals and Conferences.

Nilesh Dale obtained his Ph.D. at University of North Dakota, USA in 2009. After his Ph.D. he joined Nissan Technical Center North America to pursue fuel cell research. Currently he is Manger for Fuel Cell Research and leading the efforts on high ORR PGM and non-PGM catalyst development, durable support research, catalyst layer optimization and MEA fabrications. He has thirty publications in International Scientific Journals and Conferences and six patents.

Dr. Frédéric Jaouen obtained his Ph.D. at the Royal Institute of Technology, Stockholm, in 2003 under the supervision of Prof. Lindbergh. From 2004 to 2011, he was a research associate in Professor Dodelet's group at Institut National de la Recherche Scientifique, Canada, where he focused on non-precious metal catalysts for oxygen reduction. In 2011, Frédéric Jaouen was awarded an excellence chair from the Agence Nationale de la Recherche and moved to Université de Montpellier, France, to pursue his research on novel catalysts for electrochemical energy conversion devices as a CNRS research fellow.

Dr. Moulay-Tahar Sougrati is a CNRS Research Engineer in charge of the Mössbauer spectroscopy platform of the Charles Gerhardt Institute. He focuses on the characterization with Mössbauer spectroscopy of novel materials for energy storage and conversion. He carried out his Ph.D. on the application of ^{119}Sn Mössbauer spectroscopy to study the atmospheric corrosion of Sn-based materials (GPM, Rouen). He then

moved to Liège University (2007, 2009) where he applied ^{57}Fe Mössbauer spectroscopy to characterize metallic, organometallic and inorganic materials. Since 2009, he is involved in both the European (ALISTORE-ERI) and the French (RS2E) networks for electrochemical energy storage.

Dr. Qingying Jia is currently a Research Assistant Professor at Northeastern University. Dr. Jia obtained his Ph.D. in Material Sciences at Illinois Institute of Technology, USA in 2010. Dr. Jia's research centers on synchrotron-based *in situ* X-ray absorption spectroscopy (XAS) characterization of (electro)catalysts with applications to fuel cells and batteries.

Sanjeev Mukerjee (A brief outline) Dr. Sanjeev Mukerjee is a Professor in the Department of Chemistry and Chemical Biology (Northeastern University); where he has been since September of 1998. He also heads the newly created center for Renewable Energy Technology and its subset the Laboratory for Electrochemical Advanced Power (LEAP). He is the author of 130 peer-reviewed publications with a current H-index of 53 and is a fellow of the Electrochemical Society. He has given numerous invited and keynote presentations in various national and international meetings and holds five US and international patents. He also serves on the scientific advisory boards of three companies.

Plamen Atanassov (M.S. in Chemical Physics from University of Sofia, and Ph.D. in Physical Chemistry from the Bulgarian Academy of Sciences) is a Distinguished Professor of Chemical & Biological Engineering and Chemistry & Chemical Biology at the University of New Mexico. He is the director of the Center for Micro-Engineered Materials. Prof. Atanassov research focuses on electrocatalysis and bio-electrocatalysis and includes development of electrocatalyst for fuel cells, new materials and technologies for energy conversion and harvesting such as biological fuel cells, enzymatic and microbial as well as sensors design and integration.